FEBS Letters 498 (2001) 104–109 FEBS 24889

Functional consequences of the autosomal dominant G272A mutation in the human GLUT1 gene

Jörg Klepper[a,*], Ingrid Monden[b], Elena Guertsen[a], Thomas Voit[a], Michèl Willemsen[c], Konrad Keller[b]

[a] *Department of Pediatrics and Pediatric Neurology, University of Essen, Hufelandstr. 55, D-45122 Essen, Germany*
[b] *Institute of Pharmacology, Freie Universität Berlin, Thielallee 67-71, D-14195 Berlin, Germany*
[c] *Department of Pediatric Neurology, University Medical Center St. Radboud, P.O. Box 9101, NL-6500 HB Nijmegen, The Netherlands*

Received 1 March 2001; revised 26 April 2001; accepted 27 April 2001

First published online 10 May 2001

Edited by Judit Ovádi

Abstract The first autosomal dominant missense mutation (G272A) reported within the human GLUT1 gene and shared by three affected family members was investigated in respect to functional consequences. Substitution of glycine-91 by site-directed mutagenesis with either aspartate or alanine resulted in a significant decrease in transport activity of GLUT1 expressed in *Xenopus* oocytes. Expression of mutant transporters was confirmed by immunoblot, 2-deoxy-glucose uptake and confocal laser microscopy. The data agree with 3-*O*-methyl-glucose uptake into patient erythrocytes and indicate that the loss of glycine rather than a hydrophilic side chain (Gly91Asp) defines the functional consequences of this mutation. © 2001 Published by Elsevier Science B.V. on behalf of the Federation of European Biochemical Societies.

Key words: GLUT1; Blood–brain barrier; GLUT1 Deficiency Syndrome; *Xenopus* oocyte

1. Introduction

Transport of D-glucose across the blood–brain barrier (BBB) is mediated exclusively by the sodium-independent, facilitative transporter GLUT1 [1–3]. Focal seizures or brain injury have been shown to locally affect GLUT1-mediated glucose transport into the brain [4–7]. In contrast, a primary GLUT1 defect has recently been identified and termed GLUT1 Deficiency Syndrome or De Vivo Disease. This condition results in seizures, developmental delay and complex motor disorders in childhood [8–10]. Several heterozygous in vivo mutations have been reported in GLUT1 Deficiency Syndrome, indicating an autosomal dominant disorder resulting from GLUT1 haploinsufficiency [11–13]. The erythrocyte GLUT1 protein is identical in molecular weight and antigenic properties to the GLUT1 protein in brain capillary endothelial cells [14]. Analyses of the GLUT1 protein in patients' erythrocytes showed impaired GLUT1 function, whereas GLUT1 immunoreactivity was reduced [11] or normal [10,13].

We recently reported a father and two children from separate marriages sharing a heterozygous missense mutation (G272A) in exon 3 of the human GLUT1 gene, and presenting with clinical features of GLUT1 Deficiency Syndrome [13]. In all three individuals GLUT1 immunoreactivity of erythrocyte membranes was normal, but 3-*O*-methyl-D-glucose (3OMG) uptake into erythrocytes was significantly reduced, suggesting a quantitatively normal, but functionally impaired GLUT1 protein at the cell membrane. The predicted amino acid change (Gly91Asp) was located within an Arg-X-Gly-Arg-Arg motif between transmembrane segments 2 and 3 that is highly conserved among transporters of the major facilitator superfamily [15] and might be involved in salt-bridging between helices, in maintaining conformational stability, or in serving as a cytoplasmic anchor point for the protein [16–19]. To evaluate pathogenicity, we substituted glycine-91 with either aspartate or alanine by site-directed mutagenesis in the human GLUT1 cDNA and investigated the functional consequences using the *Xenopus* oocyte expression system. Assessment of transport rates in erythrocytes or *Xenopus* oocytes indicates that both mutations significantly reduce the catalytic activity of GLUT1.

2. Materials and methods

2.1. Mutagenesis

A 1523-bp *Bam*HI/*Bst*YI fragment of human GLUT1 cDNA derived from pSPGT [15] was subcloned into a *Bgl*II site of the *Xenopus* oocyte expression vector pSP64T [20]. Site-directed mutagenesis was carried out by polymerase chain reaction using the 'QuickChange™ Site-Directed Mutagenesis Kit' to change glycine-91 to aspartate (the native human mutation) or alanine. The mutants were confirmed by restriction fragment analysis and finally by DNA sequencing with a fluorescence DNA sequencer (ABI PRISM) connected to a Macintosh computer.

2.2. cRNA synthesis

In vitro synthesis of capped cRNA was conducted according to a standard protocol provided by Ambion (mMESSAGE mMACHINE, Ambion, Austin, USA). The amount of transcribed RNA was calculated by incorporated [^{35}S]thioUTP. Its concentration was adjusted to 0.25–0.5 mg/ml. Collection, defolliculation and culture of *Xenopus* oocytes were carried out as described previously [21,22].

2.3. Immunoblot and confocal laser microscopy

Thirty *Xenopus* oocytes injected with water (sham), wild-type GLUT1 or the indicated mutant cRNAs were selected for preparation of total membrane fractions, modified from Geering et al. [26]. The membrane fractions from the final 165 000 × *g* spin were kept at −80°C until Western blot analysis. 8 μg of protein were separated by sodium dodecyl sulphate (SDS)–polyacrylamide gel electrophoresis (PAGE) and electroblotted onto a nitrocellulose membrane by standard protocols. Membranes were stained with Ponceau S to confirm

*Corresponding author. Fax: (49)-201-723 5727.
E-mail: joerg.klepper@uni-essen.de

Abbreviations: GLUT, facilitated glucose transporter; BBB, blood–brain barrier; 2DOG, 2-deoxy-D-glucose; 3OMG, 3-*O*-methyl-D-glucose; V_{max}, maximal transport velocity; K_m, Michaelis constant

PII: S0014-5793(01)02463-2

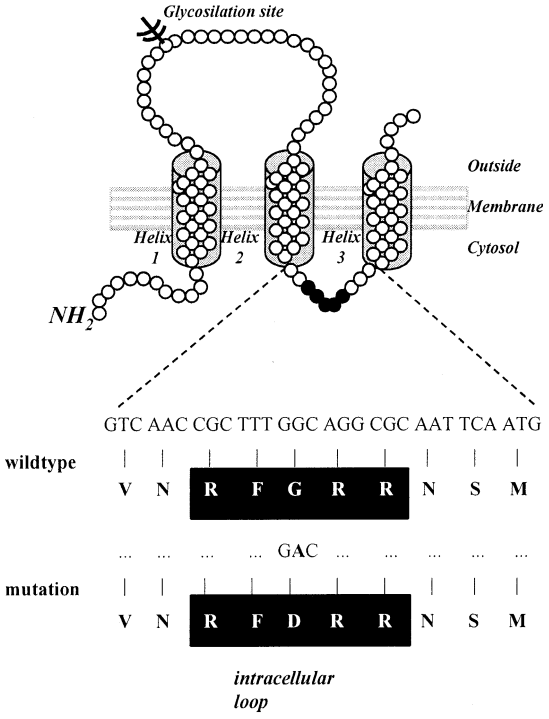

Fig. 1. The amino-terminus and helices 1–3 are shown within the conformational model for GLUT1 in the membrane as proposed by Mueckler et al. [2]. The ^{89}Arg-X-Gly-Arg-^{93}Arg motif within the intra-cellular loops joining transmembrane segments 2–3 carrying the mutation is shown in black with the nucleotide (G272A) and the amino acid (Gly91Asp) exchange indicated (adapted from [9]).

the uniform efficiency of transfer. The GLUT1 protein was identified using a polyclonal rabbit GLUT1 antibody (Cymbus Biotechnology, Chandlers Ford, Hants, UK), raised against the C-terminus of GLUT1. Primary antibodies were detected by enhanced chemiluminescence (Amersham Life Science, Arlington Heights, IL, USA). The preparation of oocytes for confocal laser microscopy followed a protocol described previously [25]. The fluorescence of three oocytes per group was scanned from the cut surface to a depth of 10 μm using the LSM 510 confocal laser scanning microscope (Carl Zeiss, Jena, Germany). The relative intensity of the plasma membrane fluorescence was divided by the average relative intensity of the cytoplasmic fluorescence. The fluorescence of the cytoplasm was scanned along a line of 40 μm from the periphery to the cell interior and was normalised to the area of the plasma membrane fluorescence. For each group, 3–4 separate oocytes per group were included in the confocal imaging.

2.4. Zero-trans 3OMG influx into erythrocytes

Zero-*trans* 3OMG influx into erythrocytes was performed as described [27]. Briefly, blood specimens were collected in citrate–dextrose–phosphate solution, immediately put on wet ice, and processed within 48 h. All procedures were performed at 4°C. Blood samples were washed three times in phosphate-buffered saline (PBS) and aliquots were incubated at increasing concentrations of [^{14}C]3OMG. Uptake was terminated, the aliquots washed twice, lysed, bleached and counted in a Scintillation Counter (Tricarb 2300, Canberra Packard, Germany).

2.5. Zero-trans 2-deoxy-D-glucose (2DOG) influx into Xenopus oocytes

The accumulation of tritium-labelled 2DOG (50 μM, 1 μCi/0.5 ml transport assay) in single *Xenopus* oocytes was assessed for 30 min at room temperature in a transport assay using 20–30 oocytes/datapoint. Kinetic data was determined over a substrate concentration ranging

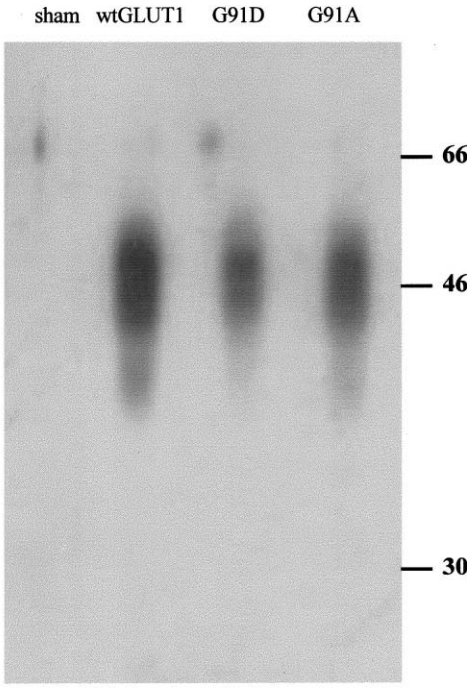

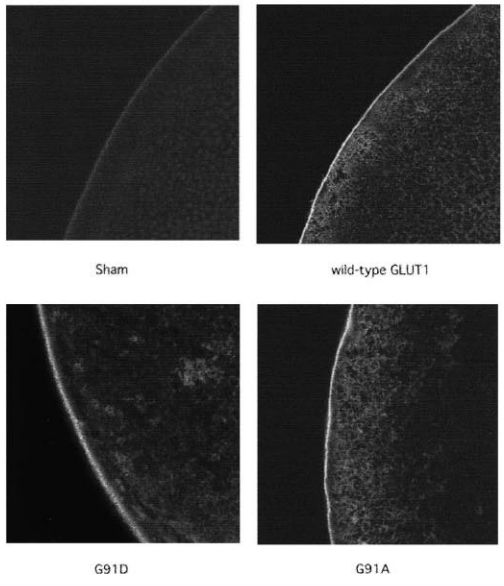

Fig. 2. Comparison of membrane glucose transporter levels by immunoblotting or confocal laser microscopy. A: Western blot analyses was conducted for *Xenopus* oocyte membranes expressing water-injected oocytes (sham) and oocytes expressing wild-type GLUT1 or the ^{91}Gly→Asp and ^{91}Gly→Ala GLUT1 mutants. Total membrane fractions were isolated as described in Section 2. Protein concentration was determined and 8 μg of protein submitted to SDS–PAGE, transferred to a polyvinylidene fluoride microporous membrane, and probed with antibodies specific for the GLUT1 carboxy-terminus. B: Confocal laser scanning microscopy was performed for *Xenopus* oocytes expressing water-injected oocytes (sham) and oocytes expressing wild-type GLUT1 or the ^{91}Gly→Asp and ^{91}Gly→Ala GLUT1 mutants. Oocytes were randomly selected, fixed and cut along the equator into two halves. An anti-GLUT1 antipeptide antibody (AK 1462; 20 μg/ml) was used as first antibody, the second antibody was a fluorescein isothiocyanate-conjugated goat anti-rabbit IgG (diluted 1:300 in PBS plus 2% horse serum). Confocal images from three to four oocytes per group were obtained by scanning the fluorescence from the cut surface to a depth of 10 μm.

from 0.5 to 25 mmol/l (i.e. 0.5, 0.7, 1.0, 2.0 and 25 mmol/l). Transport was stopped by the addition of 4°C PBS containing 0.1 mM phloretin followed by three additional washes to remove adhering radioactivity. Oocytes were dissolved in 1% SDS before radioactivity was determined by a liquid scintillation spectrophotometer [23–25].

3. Results

The G272A mutation identified in exon 3 of the human GLUT1 gene resulted in a Gly91Asp substitution within the highly conserved ^{89}Arg-X-Gly-Arg-^{93}Arg motif that is part of the first intra-cellular loop joining transmembrane segments 2 and 3 (Fig. 1).

Expression of wild-type or mutant GLUT1 transporters in total membrane fractions of *Xenopus* oocytes was investigated by Western blotting. Immunoreactivity was comparably intense for both the native and the mutant transporters (Fig. 2A). Confocal imaging focused on immunoreactivity of the transporter proteins in the plasma membrane. Mutant transporters were present at the plasma membrane at levels comparable with wild-type GLUT1 (Fig. 2B). The ratio of plasma membrane to cytoplasm fluorescence intensity was 1.21 for sham, 6.75 ± 1.20 for wild-type GLUT1 ($n = 4$), 6.62 ± 1.22 for the G91D mutant ($n = 3$) and 7.00 ± 0.86 for the G91A mutant ($n = 3$). For details, see Section 2.

Uptake values previously reported [13] in patient I:2 and II:5 (57%) and a control subject (89%), based on data of 70 normal controls [27], are shown in Fig. 3A (numbering of patients according to [13]). To evaluate saturation kinetics, zero-*trans* 3OMG influx was determined as a function of substrate concentration in erythrocytes in all patients and a control (Fig. 3B,C). Maximal transport velocity (V_{max}) was significantly reduced in all three patients compared to the intra-assay control, whereas no differences were observed for the apparent Michaelis constant (K_m) (Table 1).

Using the pSP64T-GLUT1 construct glycine-91 in the human GLUT1 cDNA was substituted by site-directed mutagenesis either with aspartate, the in vivo mutation, or alanine. Following expression of the mutant transporters in *Xenopus* oocytes 2DOG uptake rates were assessed and compared to those from water-injected and wild-type GLUT1-expressing oocytes. Both the aspartate and alanine replacement of glycine-91 resulted in a decrease in transport activity into *Xenopus* oocytes by about 40% (Fig. 3D). In *Xenopus* oocytes, the G91D and the G91A mutants showed significant reduction in both V_{max} and apparent K_m values compared to *Xenopus* oocytes expressing wild-type GLUT1 (Fig. 3E and Table 1).

4. Discussion

GLUT1 Deficiency Syndrome has been increasingly recognised as a distinct clinical entity resulting in seizures, developmental delay and complex motor disorders. As such, it represents the first known defect of transport across the BBB [8–10,28]. It can be treated effectively by means of a ketogenic diet, as ketones readily enter the brain by an independent, active transport system and serve as an alternative fuel for cerebral energy metabolism [10,29]. Mutational analyses identified a variety of private, heterozygous mutations in the GLUT1 gene in patients with GLUT1 Deficiency Syndrome [10–13]. Mutations were randomly located in various exons. In contrast to hemizygosity or non-sense mutations, the pathogenicity of missense mutations is not always clear. Mueckler et al. [38] showed that a highly conservative GLUT2 Val197Ile substitution, identified in a patient with non-insulin-dependent diabetes and expressed in *Xenopus* oocytes, abolished transport activity. This observation represented the first known dysfunctional mutation in a human facilitative glucose transporter protein [30], but the expectation that this mutation may be causally involved in the pathogenesis of non-in-

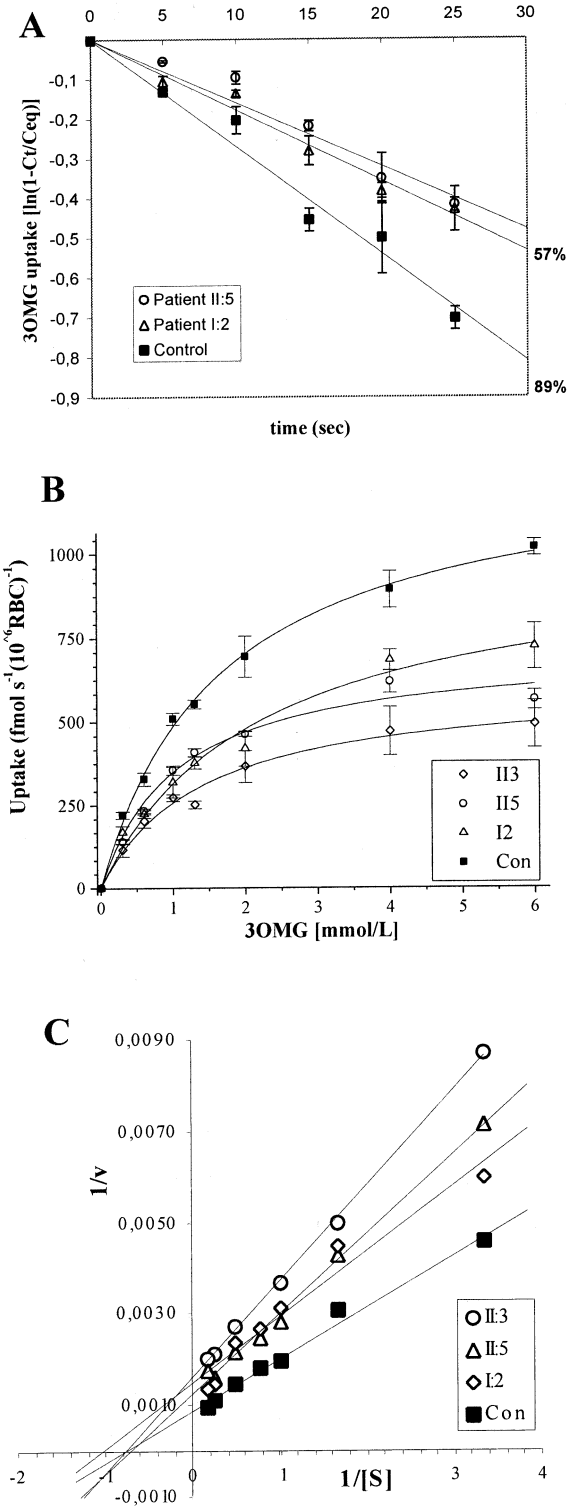

Fig. 3.

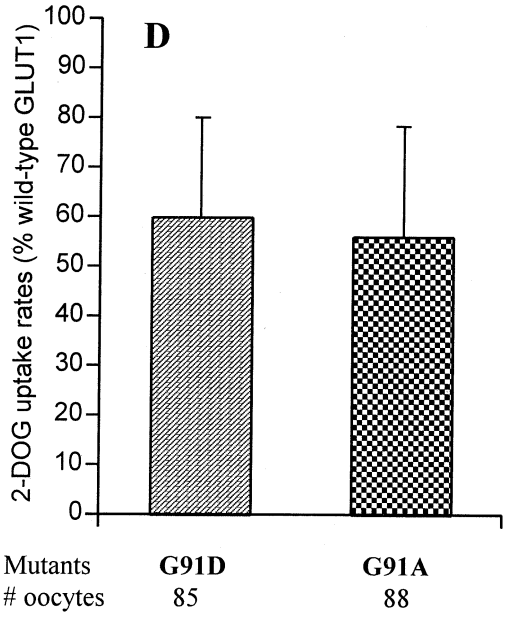

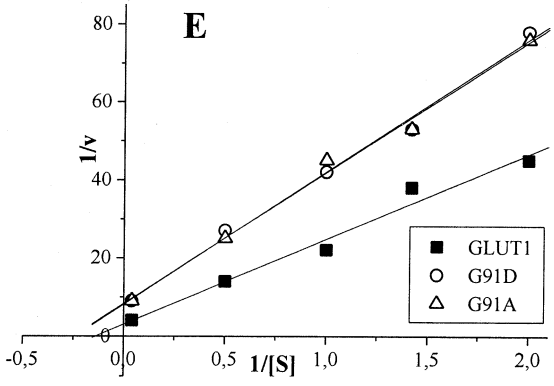

Fig. 3. Glucose transport into erythrocytes and *Xenopus* oocytes expressing wild-type GLUT1 and G91D or G91A mutant GLUT1 transporters. A: Zero-*trans* influx of 3OMG into erythrocytes over 30 s in patient II:5 and I:2. The data were expressed as the natural logarithm of the ratio of intra-cellular radioactivity at time T and at equilibrium versus time in seconds (four determinations/datapoint). The bars represent the means ± S.E.M. of relative uptake rates. The relative uptake values from both patients and the control, shown on the right y-axis, were compared to 70 controls as described in [23]. B: Saturation kinetics of 3OMG zero-*trans* influx into erythrocytes of patients and control as velocity (v) versus [S] (0.3–6 mmol/l, four determinations/datapoint). C: The data shown in (B) are presented as a double-reciprocal plot of 3OMG transport velocity (v) in fmol s^{-1} 10^6RBC^{-1} versus substrate concentration [S] in mmol/l to determine kinetic parameters shown in Table 1. D: Basal uptake rates of 2DOG into *Xenopus* oocytes. *Xenopus* oocytes were injected with cRNAs encoding the $^{91}G \rightarrow D$ or $^{91}G \rightarrow A$ mutant. The accumulation of tritium-labelled 2DOG (50 μmol/l) was assessed in single oocytes for 30 min. Each assay contained 10–15 oocytes and a separate experiment included three independent assays per group. The means ± S.D. represent the relative uptake rates from two independent experiments. The values of water-injected *Xenopus* oocytes were always subtracted. The 2DOG uptake rates by wild-type GLUT1 were 67.3 ± 20.1 pmol per oocyte × 30 min^{-1} (mean ± S.D.; $n = 90$ oocytes). E: Lineweaver–Burk plot. Kinetic analysis was performed by using groups of 20–30 *Xenopus* oocytes per datapoint to measure 2DOG uptake into oocytes expressing wild-type GLUT1 or the $^{91}G \rightarrow D$ and $^{91}G \rightarrow A$ mutants. Five different substrate concentrations were chosen to measure 2DOG influx during 30 min (15 min at 25 mmol/l substrate concentration). The values for water-injected *Xenopus* oocytes were always subtracted. ←

sulin-dependent diabetes was not confirmed in subsequent studies [31,32]. Expressing a mutant gene in *Xenopus* oocytes has since been shown to be an effective strategy to investigate the functional and structural consequences of mutations identified by molecular analyses (recent contributions: [25,33]).

The G272A mutation recently identified [13] within an ^{89}Arg-X-Gly-Arg-^{93}Arg motif, located in the first endofacial loop of GLUT1 (Fig. 1) and highly conserved among GLUT1–8, was shared by three affected family members suggesting pathogenicity. The in vivo mutation substituted glycine, a conserved small, hydrophobic and neutral amino acid, by aspartate, a long, hydrophilic and acidic, negatively charged amino acid. In addition, site-directed mutagenesis changed the glycine residue to alanine. Glycine within this motif may be involved in maintaining a certain distance between helix 1 and 2 or may support a particular orientation of the adjacent arginine residues crucial for full catalytic activity of GLUT1. Recently the substitution of the three arginine residues within the ^{89}Arg-X-Gly-Arg-^{93}Arg motif by glycine resulted in a translocation of the cytoplasmic loop into the exoplasm along with the two flanking transmembrane segments, thus completely abolishing GLUT1-mediated transport in *Xenopus* oocytes [34].

Confocal laser microscopy and immunoblotting indicated that the levels of the mutant transporters in plasma membrane or the total membrane fraction were comparable with that of wild-type GLUT1. In particular, analyses of the relative intensity of the plasma membrane versus cytoplasm fluorescence confirmed that both the wild-type and the mutant GLUT1 transporters are expressed on the cell surface.

In vitro functional analyses were performed in two different cell systems. Two independent assays investigating zero-*trans* 3OMG uptake into erythrocytes showed impaired 3OMG transport in patients (Fig. 3A–C). V_{max} values of patients and control are in agreement with previous reports [10,35]. No significant differences in apparent K_m were observed between patients and control (1.0–1.3 mmol/l), resembling the apparent K_m of 1.6 mmol/l reported in the literature for zero-*trans* influx conditions similar to those utilised here [36]. In *Xenopus* oocytes, both the G91D mutant, equivalent to the in vivo mutation, and the G91A mutant showed impaired V_{max} values, confirming the data obtained in erythrocytes. This supports the hypothesis that amino acid charges in the R-X-G-R-R motif likely play no direct role in the transport, but rather the particular amino acid and its position within the conformational structure are crucial for transport or membrane topology [34]. In contrast to the erythrocyte uptake data, the apparent K_m values were decreased in both mutants if assessed in *Xenopus* oocytes. The kinetic data for wild-type GLUT1 are in agreement with published results [36,37]. Kinetic analyses in different cell systems using substrates with different transport kinetics might be responsible for the diverging results of K_m values in *Xenopus* oocytes and erythro-

Table 1
Results of the kinetic analyses determined in erythrocytes and *Xenopus* oocytes as illustrated in Fig. 3

Sample	Age (years)	Fig. 3A	Fig. 3B,C	
		uptake (slope, %)	V_{max} ± S.D. (fmol ($s^{-1}(10^6RBC)^{-1}$))	K_m (mmol/l)
Erythrocytes:				
Pat. II:3	10	57	611 ± 35	1.3
Pat. II:5	22	–	716 ± 43	1.3
Pat. I:2	46	57	993 ± 77	1.0
Control	36	89	1275 ± 32	1.3
			Fig. 3D	
			nmol/min/oocyte	mmol/l
Oocytes:				
wt GLUT1			0.339 ± 0.25	7.4
G91D			0.126 ± 0.03	4.3
G91A			0.118 ± 0.03	3.9

cytes, however, further explanations at this point remain speculative. Analyses of further missense mutations identified in GLUT1 Deficiency Syndrome in both cell systems will be helpful to address this issue.

In summary we report the functional analysis of the first autosomal dominant mutation identified in GLUT1 Deficiency Syndrome by expression in *Xenopus* oocytes, following Mueckler's report of a dysfunctional mutation in GLUT2 [30]. We conclude that the Gly91Asp mutation within a highly conserved sequence of the GLUT1 gene highlights its importance for GLUT1 function. Since both the substitutions of glycine-91 to either aspartate or alanine led to equally impaired 2-DOG uptake rates into *Xenopus* oocytes the loss of glycine at this particular position rather than the introduction of an acidic hydrophilic side chain (Gly91Asp) defines the in vivo functional consequences of this missense mutation in the human GLUT1 gene. The data presented indicate that the heterologous expression in *Xenopus* oocytes is a useful strategy to investigate the functional consequences of in vivo mutations in human GLUT genes. Further analyses of the functional consequences of single-allele disruptions in the GLUT1 gene are necessary to unravel the genetic and biochemical background of GLUT1 Deficiency Syndrome.

Acknowledgements: The authors are grateful to Aad Verrips, University Medical Center St. Radboud, Department of Pediatric Neurology, Nijmegen, for obtaining blood samples and for helpful discussions. We further thank Christine Fischer-Lahdo and Danute Bergmann for their dedicated work as laboratory technicians, and Anne Floercken for 3OMG uptake analyses. We thank Dr. Gerd Krause, Forschungsinstitut für Molekulare Pharmakologie, Berlin, Germany, for the informative discussion on the putative structural consequences of the indicated missense mutation. This work was supported by a grant provided by the Deutsche Forschungsgemeinschaft (DFG KL 1102/2-1).

References

[1] Pardridge, W.M., Boado, R.J. and Farrell, C.R. (1990) J. Biol. Chem. 265, 18035–18040.
[2] Mueckler, M., Caruso, C., Baldwin, S.A., Panico, M., Blench, I., Morris, H.R., Allard, W.J., Lienhard, G.L. and Lodish, H.F. (1985) Science 229, 941–945.
[3] Mueckler, M., Hresko, R.C. and Sato, M. (1997) Biochem. Soc. Trans. 25, 951–988.
[4] Janigro, D. (1999) Epilepsy Res. 37, 223–232.
[5] Cornford, E.M., Hyman, S., Cornford, M.E., Landaw, E.M. and Delgado-Escueta, A.V. (1998) J. Cereb. Blood Flow Metab. 18, 26–42.
[6] Cornford, E.M., Hyman, S., Cornford, M.E. and Caron, M.J. (1996) J. Neurotrauma 13, 523–536.
[7] Cornford, E.M., Gee, M.N., Swartz, b.E., Mandelkern, M.a., Blahd, W.H., Landaw, E.M. and Delgado-Escueta, A.V. (1998) Ann. Neurol. 43, 801–808.
[8] De Vivo, D.C., Trifiletti, R.R., Jacobson, R.I., Ronen, G.M., Behmand, R.A. and Harik, S.I. (1991) N. Engl. J. Med. 325, 703–709.
[9] De Vivo, D.C., Garcia-Alvarez, M., Ronen, G. and Trifiletti, R.R. (1995) Int. Pediatr. 10, 51–56.
[10] Klepper, J., Wang, D., Fischbarg, J., Vera, J.C., Jarjour, A., O'Driscoll, K.R. and De Vivo, D.C. (1999) Neurochem. Res. 24, 587–594.
[11] Seidner, G., Garcia-Alvarez, M., Yeh, J.I., O'Driscoll, K.R., Klepper, J., Stump, T.S., Wang, D., Spinner, N.B., Birnbaum, M.J. and De Vivo, D.C. (1998) Nat. Genet. 18, 1–4.
[12] Wang, D., Kranz-Eble, P. and De Vivo, D.C. (2000) Hum. Mutat. 16, 224–231.
[13] Klepper, J., Willemsen, M., Verrips, A., Guertsen, E., Herrmann, R., Kutzick, C., Florcken, A. and Voit, T. (2001) Hum. Mol. Genet. 10, 63–68.
[14] Dick, A.P.K., Harik, S.I., Klip, A. and Walker, D.M. (1984) Proc. Natl. Acad. Sci. USA 81, 7233–7237.
[15] Baldwin, S.A. (1993) Biochim. Biophys. Acta 1154, 17–49.
[16] Gould, G.W. and Holman, G.D. (1993) Biochem. J. 295, 329–341.
[17] McGowan, K.M., Long, S.D. and Pekala, P.H. (1995) Pharmacol. Ther. 66, 465–505.
[18] Schürmann, A., Doege, H., Ohnimus, H., Monser, V., Buchs, A. and Joost, H.G. (1997) Biochemistry 36, 12897–12902.
[19] Mueckler, M. and Lodish, H.F. (1986) Cell 44, 629–637.
[20] Krieg, P.A. and Melton, D.A. (1984) Nucleic Acids Res. 14, 7057–7070.
[21] Keller, K. and Mueckler, M. (1990) Biomed. Biochim. Acta 49, 1201–1203.
[22] Garcia, J.C., Strube, M., Leingang, K., Keller, K. and Mueckler, M. (1992) J. Biol. Chem. 267, 7770–7776.
[23] Keller, K., Strube, M. and Mueckler, M. (1989) J. Biol. Chem. 264, 18884–18889.
[24] Olsowski, A., Monden, I. and Keller, K. (1998) Biochemistry 37, 10738–10745.
[25] Olsowski, A., Monden, I., Krause, G. and Keller, K. (2000) Biochemistry 39, 2469–2474.
[26] Geering, K., Theulaz, I., Verrey, F., Häuptl, M.T. and Rossier, B.C. (1989) Am. J. Physiol. 26, C851–C858.
[27] Klepper, J., Garcia-Alvarez, M., Wang, D., O'Driscoll, K.R. and De Vivo, D.C. (1999) J. Clin. Lab. Anal. 13, 116–121.
[28] Brown, G.K. (2000) J. Inherit. Metab. Dis. 23, 237–246.
[29] Nordli Jr., D.R. and De Vivo, D.C. (1997) Epilepsia 38, 743–749.
[30] Mueckler, M., Kruse, M., Strube, M., Riggs, A.C., Chiu, K.C. and Permutt, M.A. (1994) J. Biol. Chem. 269, 17765–17767.

[31] Baroni, M.G., D'Andrea, M.P., Capici, F., Buzzetti, R., Cavallo, M.G., Fallucca, F., Giovannini, C. and Pozzilli, P. (1998) Hum. Genet. 102, 479–482.
[32] Matsubara, A., Tanizawa, Y., Matsutani, A., Kaneko, T. and Kaku, K. (1995) J. Clin. Endocrinol. Metab. 80, 3131–3135.
[33] Hruz, P.W. and Mueckler, M.M. (2000) Biochemistry 39, 3967–3972.
[34] Sato, M. and Mueckler, M. (1999) J. Biol. Chem. 274, 24721–24725.
[35] Klepper, J., Fischbarg, J., Vera, J.C., Wang, D. and De Vivo, D.C. (1999) Pediatr. Res. 46, 677–683.
[36] Vannucci, S.J., Maher, F. and Simpson, I.A. (1997) Glia 2, 2–21.
[37] Bell, G.I., Burant, C.F., Takeda, J. and Gould, G.W. (1993) J. Biol. Chem. 268, 19161–19164.
[38] Mueckler, M., Wenig, W. and Kruse, M. (1994) J. Biol. Chem. 269, 20533–20538.